Steered Molecular Dynamics Simulations of Na^+ Permeation across the Gramicidin A Channel

Zhanwu Liu,[†] Yan Xu,[†,‡] and Pei Tang*[,†,‡]

Departments of Anesthesiology and Pharmacology, School of Medicine, University of Pittsburgh, Pittsburgh, Pennsylvania 15260

Received: February 1, 2006; In Final Form: April 21, 2006

The potential of mean forces (PMF) governing Na^+ permeation through gramicidin A (gA) channels with explicit water and membrane was characterized using steered molecular dynamics (SMD) simulations. Constant-force SMD with a steering force parallel to the channel axis revealed at least seven energy wells in each monomer of the channel dimer. Except at the channel dimer interface, each energy well is associated with at least three and at most four backbone carbonyl oxygens and two water oxygens in a pseudo-hexahedral or pseudo-octahedral coordination with the Na^+ ion. Repeated constant-velocity SMD by dragging a Na^+ ion from each energy well in opposite directions parallel to the channel axis allowed the computation of the PMF across the gA channel, revealing a global minimum corresponding to Na^+ binding sites near the entrance of gA at ±9.3 Å from the geometric center of the channel. The effect of volatile anesthetics on the PMF was also analyzed in the presence of halothane molecules. Although the accuracy of the current PMF calculation from SMD simulations is not yet sufficient to quantify the PMF difference with and without anesthetics, the comparison of the overall PMF profiles nevertheless confirms that the anesthetics cause insignificant changes to the structural makeup of the free energy wells along the channel and the overall permeation barrier. On average, the PMF appears less rugged in the outer part of the channel in the presence of anesthetics, consistent with our earlier finding that halothane interaction with anchoring residues makes the gA channel more dynamic. A causal relationship was observed between the reorientation of the coordinating backbone carbonyl oxygen and Na^+ transit from one energy well to another, suggesting the possibility that even minute changes in the conformation of pore-lining residues due to dynamic motion could be sufficient to trigger the ion permeation. Because some of the carbonyl oxygens contribute to Na^+ coordination in two adjacent energy wells, our SMD results reveal that the atomic picture of ion "hopping" through a gA channel actually involves a Na^+ ion being carried in a relay by the coordinating oxygens from one energy well to the next. Steered molecular dynamics complements other computational approaches as an attractive means for the atomistic interpretation of experimental permeation studies.

Introduction

Both structurally and functionally, gramicidin A (gA) is one of the best characterized ion channels.[1−5] It comprises a head-to-head $\beta^{6.3}$ dimer with alternating L and D amino acids in each monomer, having the sequence of HCO-L-Val^1-Gly^2-L-Ala^3-D-Leu^4-L-Ala^5-D-Val^6-L-Val^7-D-Val^8-L-Trp^9-D-Leu^{10}-L-Trp^{11}-D-Leu^{12}-L-Trp^{13}-D-Leu^{14}-L-Trp^{15}-$NHCH_2CH_2OH$. The hydrogen bonds formed between the backbone amide hydrogen and the carbonyl oxygen extend parallel to the pore axis and stabilize a transmembrane (TM) channel that is ∼25 Å long from Trp^{11} to Trp^{11} oxygens in the dimer, with a pore diameter of ∼4 Å. The availability of high-resolution structures and other experimental data makes gA an excellent model system to study ion permeation across a TM channel.[6,7]

The permeation process across a gA channel has been conceptualized as consisting of at least four energetically distinguishable steps: diffusion of an ion from the bulk solvent to the entrance of the channel, dehydration and binding of the ion within the channel, translocation across the channel, and rehydration and departure from the channel into the bulk solvent.[7,8] All experimental analyses seem to agree that the binding sites for monovalent ions are near the channel entrances, but the precise location varies among different measurements. In the four permeation steps, the translocation from one end of the channel to the other end is perhaps the least understood step from the molecular viewpoint. Because of the lack of experimental details, this step is often simplified to a central energy barrier with respect to the ion movement along the so-called reaction pathway. Although a significant amount of new knowledge has been gained in the past two decades, the details of the actual steps for monovalent cations to bind and to move through the >18-Å-long pore still require further elucidation.[9] A glimpse of the atomistic picture of translocation can sometimes be obtained from molecular dynamics (MD) simulations.[8,10,11] However, traditional MD simulation is often hindered by the short time scale incompatible with the biological processes. In the case of Na^+ permeation in the gA channel, the characteristic time is typically on the order of hundreds of nanoseconds or longer, beyond the current computation limit of all-atom MD simulations. The umbrella sampling method has been used recently to capture the energetics of the ion permeation process.[12,13] The steered molecular dynamics (SMD)

* Author to whom correspondence should be addressed. Phone: (412) 383-9798. Fax: (412) 648-8998. E-mail: tangp@anes.upmc.edu.
† Department of Anesthesiology.
‡ Department of Pharmacology.

10.1021/jp060688n CCC: $33.50
Published on Web 06/03/2006

simulation, where a biological system is steered by applying a moving constraint, is another attractive way to overcome the difficulties related to the unrealistically long time scales faced by the traditional MD simulations and to explore the biological process at the submolecular level.[14−17]

Another interesting area of research related to ion permeation across gA is to use this structurally well-defined channel as a model to yield insights into the molecular mechanisms of action of general anesthetics. A series of experimental and computational investigations[18−23] have led to an in-depth understanding of anesthetic interaction with channel proteins. These studies suggest that anesthetics at physiologically relevant concentrations can only produce minor changes in channel structures but have a profound impact on channel dynamics.[20−22] These findings validate the notion that dynamic characteristics of channel motions are of functional significance. One of our NMR experimental studies demonstrated that anesthetic molecules interacted with Trp residues at the peptide−lipid−water interface and that the presence of anesthetic molecules increased the Na^+ permeation rate by ~25%.[19] These experimental findings prompted us to further pursue computational studies of Na^+ permeation across the gA channel, focusing mainly on the submolecular details of ion−peptide interaction at the binding site and during the translocation process.

We present here the SMD simulations of Na^+ permeation across the gA channel in a fully hydrated dimyristoylphosphatidylcholine (DMPC) membrane in the absence and presence of anesthetic halothane. The main goal is to elucidate the actual backbone and side-chain dynamics occurring in the gA channel as a Na^+ ion is cruising through the channel pore. Although the current accuracy of calculating the potential of mean force (PMF) of ion permeation from SMD simulations is not sufficient to quantify the anesthetic-induced difference in the PMF, a comparative study is nevertheless expected to provide a qualitative energetic description regarding the anesthetic effects on the actual steps constituting the translocation process, thereby shedding new light on the understanding of how anesthetics modulate the ion channel functions in general.

Methods

System Preparations. The starting systems for SMD simulations were modified from our previous systems in the presence and absence of anesthetic halothane after 2.2-ns MD simulations.[22] Excess lipids in the original systems were removed to reduce the computational cost. The final systems for the current study have 1 gA channel (PDB code 1MAG[24]), 64 DMPC lipids, 2642 TIP3 water molecules, and 1 Na^+/Cl^- pair. For the system with halothane, 10 TIP3 water molecules are replaced by 10 halothane molecules. The channel *Z*-axis is parallel to the membrane normal (Figure 1), and the pore of the channel is filled with single-file water molecules. After the energy minimization with a conjugate gradient for 5000 steps, the two systems with and without halothane were each subjected to 200-ps constant pressure and temperature (NPT) equilibration at 305 K and 1 bar using the Nosé−Hoover method.[25,26] The Langevin dynamics was used to keep the temperature constant without coupling the steered Na^+ to the temperature bath. The cutoff distance for van der Waals interaction was 12 Å, with the pair list distance extended to 13 Å. A periodic boundary condition was imposed. The long-range full electrostatic interactions were evaluated every four time steps using the particle mesh Ewald method.[27] The SHAKE routine was used in all simulations to restrain all bonds between hydrogen and its parent atom within a tolerance of 10^{-6} Å.[28]

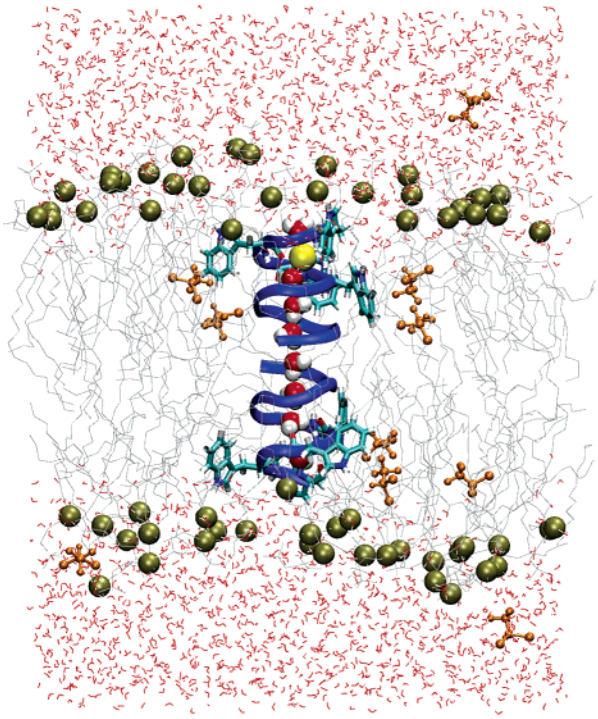

Figure 1. Snapshot of the simulation system in the presence of halothane. The system consists of a gA channel (backbone shown as blue ribbons and Trp side chains as cyan bond representations), 64 DMPC lipids (alkyl chains shown as gray lines and phosphorus atoms as golden spheres), 2462 water molecules, Na^+ (yellow sphere inside the channel) and Cl^- (in the bulk water but not shown), and 10 halothane molecules (orange).

The system preparations and simulations were performed on either the Cray T3E or the HP GS128 at the Pittsburgh Supercomputing Center using the NAMD2 program[29] with the CHARMM22 force field.[30,31] The VMD program was used for visualization and data analysis.[32]

Steered Molecular Dynamics Simulations. Both constant-force SMD (cf-SMD) and constant-velocity SMD (cv-SMD) simulations were conducted. In a cf-SMD scheme, Na^+ was initially placed at the entrance of the gA channel (14 Å from the geometry center on the channel axis) by replacing a TIP3 water molecule and was restrained in the subsequent 1000-step energy minimization and 100-ps NPT equilibration. Thereafter, a constant force of 2.16 kcal/(mol Å) was applied to the Na^+ ion to pull it in the *Z*-direction (parallel to the channel axis) from the mouth to the center of the channel, while no restraint was imposed on the ion in the *X*−*Y*-directions. The *Z*-coordinates with long ion dwelling time were identified from cf-SMD simulations, and each of these dwelling positions was then used as the center point for two sections in the subsequent cv-SMD simulations. For cv-SMD simulations, a harmonic constraint of 20 kcal/(mol Å^2) was first applied to the Na^+ to keep it at each selected dwelling position while the system underwent 1000-step energy minimization and 100-ps equilibration. Thereafter, the constraint was removed, and the Na^+ ion was pulled in both +*Z*- and −*Z*-directions at constant velocities of +0.01 and −0.01 Å/ps. The cv-SMD scheme consists of many independent 150−300 ps simulations so that the trajectories from each section overlap with those of the adjacent, opposite-pulling sections defined by the two neighboring dwelling points. To ensure that the reaction coordinate for the one-dimensional (1D) PMF remains parallel to *Z*, the *Z*-coordinates of backbone atoms of the gA channel were constrained using a small force constant of 0.5 kcal/(mol Å^2)

to prevent channel tilting and drifting. Up to 28 independent cv-SMD sections across the channel were conducted (see below for details). In each section, cv-SMD simulations were repeated at least eight times for ensemble averaging and for smoothing out variations due to possible "hysteresis" in the opposite-pulling directions.[8] The total simulation time for the cv-SMD scheme was about 40 ns for each system.

Potential of Mean Force Reconstructions. It has been suggested[13,33] that for an ion within the narrow pore of the gA channel the motions in the $X-Y$-directions reach equilibrium very rapidly. Thus, the dependence of the PMF on X and Y can be integrated away.[13] The reconstruction of the 1D PMF using the results of cv-SMD simulations follows the principle of Jarzynski's equality,[34] which theorizes the possibility of calculating equilibrium properties from nonequilibrium simulations and establishes a link between the nonequilibrium work and the equilibrium free energy changes. A realistic PMF reconstruction method using a limited number of cv-SMD trajectories has been developed recently[17,35] and adopted in this study. For each section along the channel, the trajectories of the force experienced by the sodium ion and the ion coordinates were normally divided into many 10-ps windows; the averaged ion position $\bar{z}(j)$ and work $\bar{W}(j)$ within the jth window were calculated and used in eq 1 for PMF calculations in each section

$$G(\langle\bar{z}(j)\rangle) = \langle\bar{W}(j)\rangle - \frac{\beta}{2}[\langle\bar{W}(j)^2\rangle - \langle\bar{W}(j)\rangle^2] \qquad (1)$$

where the brackets denote ensemble average, $\beta = 1/kT$, k is the Boltzmann constant, T is the temperature of the simulation (305 K), and $\langle\bar{W}(j)^2\rangle$ is defined as

$$\langle\bar{W}(j)^2\rangle \equiv \frac{1}{N}\sum_n\left\{\int\frac{dt}{\Delta t}\left[W_n(t) - \frac{k}{2}(\langle\bar{z}(j)\rangle - z_0 - v\bar{t}(j))^2\right]\right\}^2 \qquad (2)$$

where $\bar{t}(j)$ is the middle time point of the jth window, $v = \pm 0.01$ Å/ps, and N is the number of trajectories. The PMF of the full channel was assembled from the sectional PMFs using the published method.[17]

Results and Discussion

Estimation of Na^+ Permeation Energetics Using cf-SMD. Despite the fact that a constant pulling force (2.16 kcal/(mol·Å)) was applied to Na^+ in the cf-SMD simulations, the ion moved in discrete instead of continuous steps in the Z-direction from one position to the next, as shown in Figure 2. This is the case when the harmonic force constant is comparable to or slightly smaller than the averaged slope of the PMF changes from the local minima to the adjacent barriers, thereby yielding a rough estimation of the 1D locations of energy peaks and wells along the channel. At least seven dwelling positions, at ~11.4, 9.3, 7.7, 6.3, 4.7, 2.7, and 0.7 Å from the dimer center, were identified in the cf-SMD simulations. The dwelling position at 7.7 Å is more clearly defined in the system with than without halothane (Figures 2 and 3). All of the dwelling positions along Z-axis should roughly correspond to the local 1D PMF minima. It is conceivable that if the applied constant force is carefully adjusted, then it is possible to relate the Na^+ resident time at dwelling positions to the relative height and slope of local energy barriers in the PMF, providing a quick way to qualitatively estimate the free energy profile of ion permeation.

Potential of Mean Force from cv-SMD. Figure 3 shows the PMFs for a Na^+ ion permeating through the gA channel in the absence and presence of anesthetic halothane molecules.

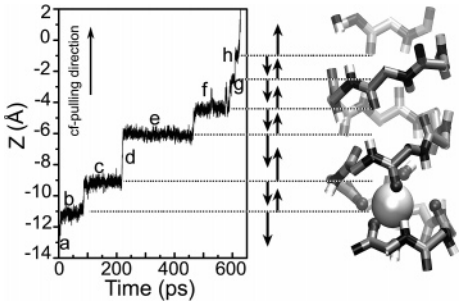

Figure 2. Left: Na^+ Z-coordinates from the SMD trajectory under constant force (2.16 kcal/(mol·Å), or ~150 pN) pulling from the entrance ($Z = -14$ Å) to the geometric center ($Z = 0$) of the channel in the absence of halothane molecules. The glitch at 7.7 Å, which is difficult to see on a full time scale, is visible when the region is expanded and even more clearly defined in the cf-SMD trajectory with halothane (data not shown). Right: Snapshot of cf-SMD, showing Na^+ coordination by four carbonyl oxygens from the gA backbone. Two additional points of coordination, above and below Na^+, are provided by the oxygen of the water in the pore. Middle: Na^+ dwelling positions defined as the starting points for two directional cv-SMD simulations, as indicated by the arrows in the middle column of the figure.

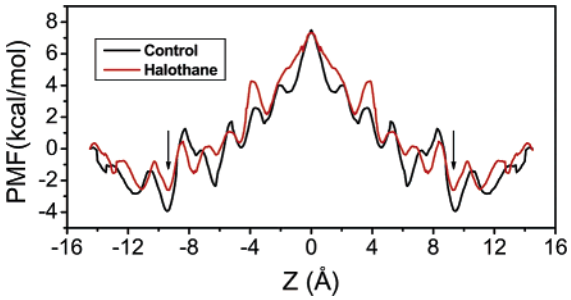

Figure 3. Potential of mean force reconstructed from cv-SMD (±0.01 Å/ps) simulations for Na^+ permeation across a gA channel in the presence (red) and absence (black) of halothane molecules. The vertical arrows mark the Z-positions of the global PMF minima corresponding to the Na^+ binding sites at the entrances of the channel pore ($Z = \pm 9.3$ Å).

Each PMF curve was reconstructed from averaging at least 8 repeated cv-SMD simulations over up to 28 sections starting from the 14 energy wells in the dimer. In the system without halothane, equilibration at ±7.7 Å before cv-SMD simulations always resulted in the ion being at the adjacent dwelling positions, and therefore, only 12 energy wells (24 sections) were used for the PMF reconstruction in the absence of halothane. The final PMFs were symmetrized relative to the dimer center along the Z-direction.

Several features in the PMFs are worth mentioning. First, the number of energy minima and their locations along the gA channel are in good agreement between the two, indicating that the structural compositions of the local energy wells along the channel are essentially unaffected by the anesthetics. Particularly, the main Na^+ binding sites (the global PMF minima) are at $Z = \pm 9.3$ Å regardless of whether the halothane is present or not, and the corresponding depths of the energy wells are −3.9 and −2.4 kcal/mol in the absence and presence of halothane, respectively. Although the difference between the two values is nonessential given that it is within the current range of accuracy for PMF calculations from SMD simulations, the trend (i.e., a slight elevation in the PMF due to halothane) is nevertheless consistent with the expected change in dipolar interaction between Na^+ and Trp side-chain orientations at this location. We have shown experimentally that halothane interacts specifically with the anchoring Trp side chains at the lipid−water interface.[21] As discussed below, this interaction is believed

to increase the probability of side-chain reorientation, thereby altering the binding energetics at the ion-binding sites.

The second PMF feature is that the height of the central barrier related to the PMF at the entrance of the channel is not affected by anesthetics, albeit on average the 1D PMF along Z appears slightly less rugged on the outer part of the channel. The third feature is that the local energy minima occur with a periodicity of ~1.6 Å along the channel. This periodicity coincides with the coordination of the carbonyl oxygen from the channel backbone and will be discussed further later.

It is expected that the systems with and without halothane have similar PMFs. Our previous NMR measurements with gA in phosphatidylcholine/phosphatidylglycerol vesicles at 298 K showed that the rate of Na^+ transport across a gA channel increased from $k_i^{control} = 182\ s^{-1}$ under the control condition to $k_i^{F3} = 223\ s^{-1}$ after the addition of anesthetic F3.[19] If a simple kinetic model is used for a *qualitative* estimation, then the corresponding change in the free-energy barrier to Na^+ transport is only 0.12 kcal/mol, provided that the Eyring "frequency factor" remains unchanged

$$\Delta\Delta G^{\ddagger} = -RT \ln\left(\frac{k_i^{control}}{k_i^{F3}}\right) \quad (3)$$

The anesthetic effects from halothane and F3 can be safely assumed to be similar.[21,36] Thus, within the current PMF calculation accuracy limit, it is consistent with the experimental results that the overall PMF barrier is unchanged in response to halothane perturbation. The similarity of the two PMF profiles in Figure 3 of two systems of different starting configurations, with combined total simulation time more than 80 ns, can be taken as an indication that cv-SMD simulations with different random seeds are at least internally consistent for calculating PMFs.

The PMFs from cv-SMD simulations also give reasonable prediction of the location of the primary Na^+ binding site. Earlier NMR experiments based on chemical shift perturbation to the selectively ^{13}C-labeled gA placed the binding sites at ~11.5 Å from the center of the channel dimer,[37] which is within the first helix turn at the mouth of the channel. However, because many factors can affect NMR frequencies in a complicated way, net chemical shift changes alone are neither necessary nor sufficient indicators of ion binding. X-ray diffraction suggested that the monovalent binding site is deeper in the channel, about 9.6 Å from the center, or right below the first helix turn.[38] More recently, studies by MD simulations in comparison with the chemical shift anisotropy data from solid-state NMR placed the main binding site further in the channel at ~9.2 Å from the center.[39] The global minima of PMFs in this study indicate that the ion-binding sites are at ±9.3 Å from the dimer center, in reasonable agreement with the X-ray and solid-state NMR results.

Aside from the binding site location, the predictions of Na^+ binding energy and the overall energy barrier to Na^+ transport, however, are rather controversial. On the basis of the absolute reaction rate theory,[40] our previous NMR measurements suggested that the free energy of activation for Na^+ influx was ~8.2 kcal/mol.[19] The Na^+ binding energy and activation enthalpy (ΔH) from another NMR experiment[41] are −2.1 and 5.4 kcal/mol, respectively. The theoretical fittings of single-channel data showed the binding energy of −3.1 kcal/mol (−5.3kT) and the barrier height of 2.1 kcal/mol (3.6kT).[42,43] Because of the intrinsic uncertainty of the PMF in the region close to the bulk water and the lack of a reliable bulk reference,

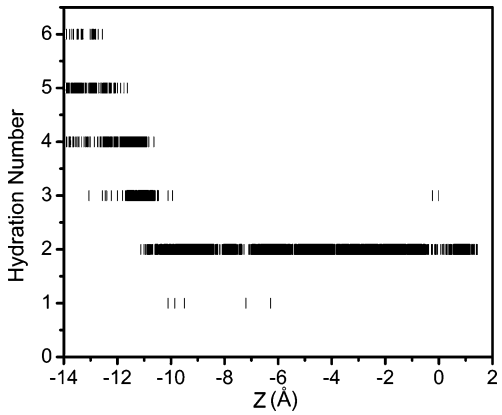

Figure 4. Na^+ hydration numbers as a function of Na^+ location along the Z-axis. Water molecules, whose oxygen atoms are within 3 Å of Na^+, are considered to be the ion-coordinating molecules contributing to Na^+ hydration. As Na^+ enters the channel, the hydration number reduces from 6 to 2.

the absolute value of the binding energy is difficult to define in the current study. However, the depth of the global energy well of −3.9 kcal/mol (or −2.4 kcal/mol in the presence of halothane) from the current study agrees reasonably well with these experimental binding energies. The central energy barrier seems to have been overestimated. Similar overestimations were also found in an early MD simulation, in which the binding energy and the barrier height were −7.0 and 6.8 kcal/mol, respectively.[8]

The discrepancy between experimentally and computationally determined translocation energy (reflected as the central barrier height) has been noticed for some time. It is generally agreed that the accuracy of simulations on free energy profiles of ion permeation suffers from two limitations.[10] First, electronic polarization is not treated appropriately in the current force field used for MD simulations. Second, periodic boundary conditions may interfere with the long-range electrostatic contributions. The magnitude of artifacts due to periodicity and the lack of hydrocarbon polarizability was estimated to be ~3.7 kcal/mol in a recent MD simulation on the energetic profile of K^+ conduction through the gA channel, where the correction of the artifact was elegantly demonstrated.[13] The replacement of periodic boundary conditions with slab geometric boundary conditions has shown promising results.[44] A force field with better electronic polarization properties is also expected to improve the accuracy in the determination of the energy profile for ion permeation across gA channels as well as other ion channels. A semi-microscopic approach that circumvents the above two limitations has shown an impressive agreement between the calculated results and the experimental measurements.[10]

Na^+ Interaction with Water and Gramicidin A Carbonyls. The Na^+ interaction with water and carbonyls of the gA backbone is certainly one of the most crucial elements for Na^+ permeation. Figure 4 depicts the dehydration process of Na^+ from bulk water into the gA channel. The ion-coordinating water molecules, whose oxygen is within 3 Å of Na^+, are reduced progressively from 6 to 2 when Na^+ moves from the outside to the inside of the channel. It is noteworthy that Na^+ dehydration starts at an entry location, 14 Å away from the geometric center of the channel. Three water molecules are coordinated with Na^+ transiently at the center of the channel (i.e., at the dimer interface), presumably because of more flexible space between the two monomers. As shown in Figure 4, Na^+ is coordinated by two water molecules at the binding site as well as in the interior of the channel. These observations are consistent with

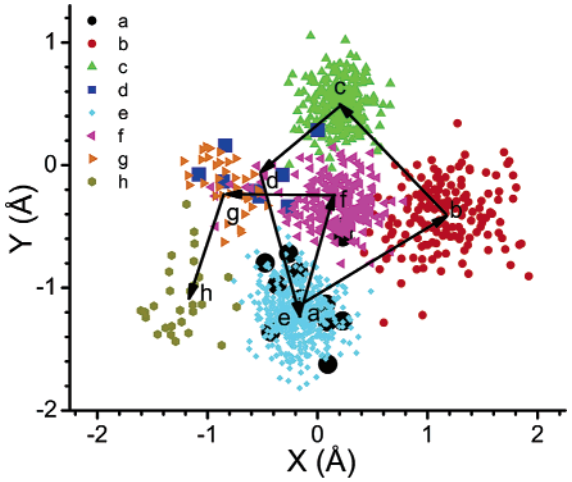

Figure 5. *X*−*Y*-coordinates of Na^+ ion recorded at 1-ps intervals inside a gA channel during cf-SMD simulations. Different *Z*-dwelling positions (Figure 2) are distinguished by different colors of the symbols. Notice the off-axis clustering and the zigzag pathway from one cluster center to the next.

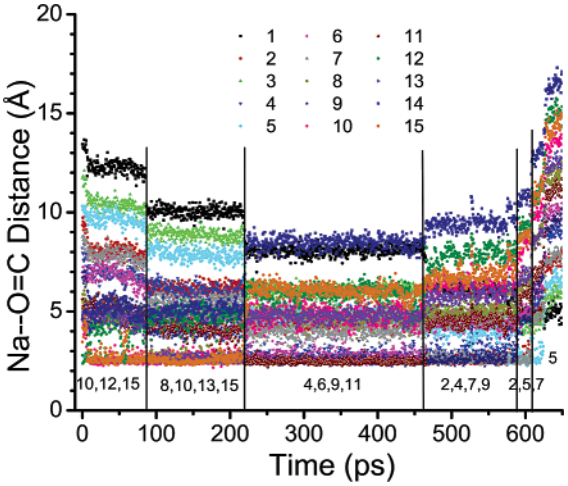

Figure 6. Distances from the Na^+ ion to all carbonyl oxygens of the 15 residues in one monomer of gA recorded with 1-ps temporal resolution during cf-SMD simulations. Numbers 1−15 in the figure refer to the residue numbers. Because the ion moves in discontinuous steps, the distances exhibit distinct bands. Expansion of the vertical scale around 2.5 Å allows positive identification of residues contributing to the coordination at each dwelling position. Notice that the shortest distance band remains constant (about ∼2.5 Å) throughout the channel and that the Na^+ ion is at a quasi-equal distance to the coordinating carbonyl oxygen at all dwelling sites.

the results for K^+ in the gA channel determined by umbrella sampling.[13] Experimental observation of stepwise dehydration has been reported.[45,46]

Besides being coordinated by oxygen atoms of two water molecules inside the channel, Na^+ also interacts snuggly with the backbone carbonyl oxygens. Figure 5 depicts the Na^+ *X*−*Y*-coordinates recorded at 1-ps intervals during the cf-SMD simulations. It can be seen clearly that at each *Z*-dwelling position, the *X*−*Y*-coordinates of Na^+ are clustered off the channel axis. The centers of the clusters are as large as ∼1.3 Å away from the axis. This result validates the speculation from an earlier computation study suggesting that small ions tend to lie off-axis in the channel pore to achieve better solvation.[47] More recent computation studies also showed that ions are lying off-axis at the binding site near the channel entrance.[48] Our cf-SMD simulation shows that even though the pulling force is applied only in the *Z*-direction, the Na^+ ion "hops" along a zigzag off-axis path as shown in Figure 5. Careful examination of Na^+ solvation at each *Z*-dwelling position indicates that except at the dimer interface Na^+ is well coordinated by at least three and at most four gA backbone carbonyl oxygens in addition to the two water oxygens in a pseudo-hexahedral (i.e., pentacoordinate in a triangular dipyramid) and pseudo-octahedral (i.e., hexacoordinate in a square dipyramid) arrangement, respectively. Figure 6 shows the distances of Na^+ to the backbone carbonyl oxygens in the Na^+-containing monomer during the cf-SMD simulations. Consistent with the "quantized" movement of the ion in the channel on the picosecond time scale, the distances in this figure are also clustered in distinct bands. Notice, however, that the shortest distances are clustered around 2.5 Å and are invariant throughout the channel. Thus, even at other dwelling sites outside the energetically defined ion-binding site, the sodium ion is coordinated at a quasi-equal distance to the coordinating carbonyl oxygens.

Because of the discrepancy among various experimental methods about the precise location of the ion-binding site, the atomistic details of the interaction between the ion and the channel at the binding site are not entirely clear. It was suggested earlier that Trp^9, Trp^{11}, and Trp^{13} carbonyls might be involved in ion coordination.[37] Later solid-state NMR measurements were interpreted as suggesting that cations were solvated at the binding site by no more than two carbonyls and no fewer than three water molecules at any time.[45] Computational analyses reasoned that ions at the binding site are lying off-axis and solvated by Leu^{10} and Trp^{11} carbonyls and two single-file water molecules, one before and one after the ion in the channel.[48] Our SMD simulations yielded a more complete picture of ion coordination within the gA channel. Expanding the vertical region near 2.5 Å in Figure 6 reveals that the coordinating residues at the first six dwelling positions involve (L10, L12, W15), (V8, L10, W13, W15), (V6, V8, W11, W13), (L4, V6, W9, W11), (G2, L4, V7, W9), and (G2, A5, V7). It should be noted that because the ion residence at 7.7 Å is less defined in the absence of halothane the residues for this site are first inferred from the coordination at the preceding and succeeding dwelling positions and later confirmed by the cf-SMD simulations in the presence of halothane, in which the energy well at 7.7 Å is clearly defined (Figure 3). It should also be noted that coordinating residues are shared in pairs by the adjacent energy wells. For example, V8, L10, W13, and W15 are involved in the coordination at the main ion-binding site. Of the four residues, L10 and W15 also contribute to the coordination at the preceding dwelling site, whereas the other two residues, V8 and W13, contribute to the coordination at the succeeding dwelling site. Thus, even though the ion translocation appears to be "hopping" from one dwelling site to the next on the picosecond−nanosecond time scale (Figures 2 and 5), the ion movement is more appropriately viewed dynamically as being "carried" by the coordinating carbonyls from one coordinating site to the next in a series of relays. This is the first time such submolecular details of ion translocation inside a channel are revealed, which may prove to be useful to reconcile the differences between the chemical kinetics model and the continuum electrodiffusional model for analyzing ion permeation.[49]

The finding that the distance from Na^+ to the coordinating carbonyl oxygens is constant at all local PMF minima is important. It suggests that the enthalpic contribution to the PMFs from the direct interaction between Na^+ and the carbonyl oxygen is essentially the same at the channel entrance, main ion-binding site (which is fully occupied at high ion concentrations), and

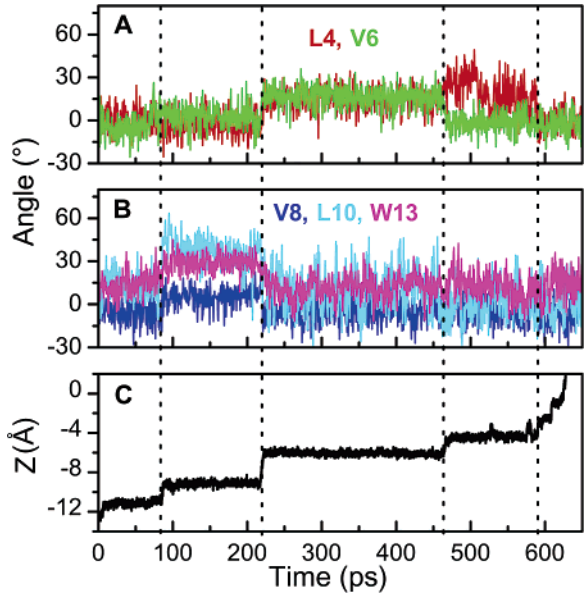

Figure 7. Correlation between backbone carbonyl orientation and the coordination with Na^+. The orientation angles are defined as deflection from the channel *Z*-axis. (A) L4 and V6 carbonyl bonds are deflected to coordinate with Na^+ at 6.3 Å. As Na^+ hops to 4.7 Å, L4 remains deflected, but V6 is no longer coordinated with Na^+. (B) As Na^+ hops to 9.3 Å, L4 and V6 are relaxed while V8, L10, and W13 are deflected. (C) Corresponding Na^+ trajectory from a cf-SMD simulation.

other dwelling locations inside the channel. The reason that dwelling sites other than the main ion-binding site are not detected by experimental methods such as NMR chemical shift anisotropy measurements is because these other sites are unoccupied most the time at equilibrium. Because the enthalpy of local interaction is invariant at all dwelling sites, the global energy minima and translocation probability are thus likely controlled by the long-range interactions, such as dipolar interaction with the side chains or lipid bilayers, and by the entropic contributions from the number of thermally accessible states at the various dwelling locations.

It has been a subject of debate as to whether interaction between Na^+ and carbonyls causes any gA structure deformation.[39,50,51] Some believe that conformational changes in the backbone of gA are insignificant upon cation binding,[51] whereas others contend that the displacement of gA atoms is essential to prepare a pathway for the movement of Na^+ ion.[50] Strong correlation between carbonyl movement and Na^+ position can be clearly visualized in our cf-SMD simulations in the present study. As shown in Figure 7, the vectors connecting carbonyl carbon and oxygen deflect away from the normal direction parallel to the channel axis (*Z*-axis) when Na^+ becomes in contact with the carbonyls and resides at the binding site (V8, L10, and W13) or at other local energy minima (for example, V6 and L4 at 6.3 Å). The deflection angle upon Na^+ contact can be as large as ~20°, implicating considerable flexibility that can potentially induce local deformation of channel backbone. At the expenses of negative entropy, such strongly coupled, concerted interaction is required to facilitate Na^+ movement from one position to the next.

Orientations of Tryptophan Residues. Many lines of experimental evidence indicate that Trp residues are critical to the function of the gA channel.[52−56] In addition to their role as anchoring residues at the lipid−water interface to stabilize the channel in the transmembrane orientation, Trp residues at the entrance region of gA are important for ion permeation through noncontact dipole effects. It has been shown that the channel

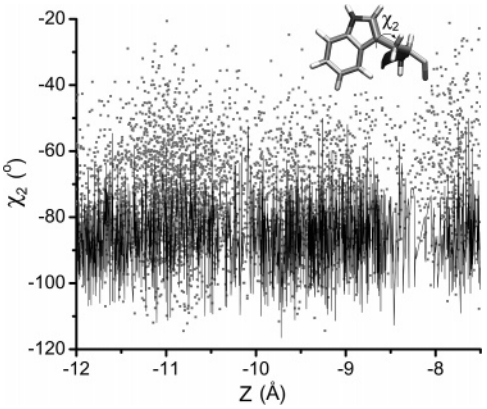

Figure 8. Comparison of dihedral angle χ_2 of W15 as a function of Na^+ position in the absence (black lines) and presence (grey dots) of halothane. χ_2 is defined in the insert. Notice the significantly wider spread of χ_2 and the shift of the mean in the presence of halothane. The data shown were from four repeats of two separate cv-SMD simulations, starting at $Z = 9.3$ Å and steering in opposite directions toward the entry and the center of the channel.

TABLE 1: Averaged Dihedral Angles of Tryptophan Side Chains of Gramicidin A in the Control and Halothane Systems from 4 to 10 Repeated cv-SMD Simulations

residue angle	control	halothane
W9 χ_1	-62.1 ± 7.1	-63.0 ± 9.3
W9 χ_2	-75.9 ± 10.0	-77.6 ± 12.0
W11 χ_1	-66.6 ± 9.2	-59.7 ± 8.6
W11 χ_2	-88.5 ± 10.9	-76.1 ± 12.7
W13 χ_1	-58.2 ± 7.7	-60.4 ± 8.9
W13 χ_2	-84.8 ± 11.1	-85.8 ± 12.3
W15 χ_1	-62.1 ± 7.4	-58.1 ± 9.3
W15 χ_2	-86.0 ± 10.2	-70.9 ± 15.0

conductance can be modulated by modification of electrical dipole potentials from side chains of Trp, upon either replacement of Trp with a nonpolar amino acid or indole fluorination.[53−56] The orientation of Trp side chains affects the orientation of the dipole moment and ultimately imposes effects on lowering the overall free energy at the ion-binding site and hence the ion permeation. Table 1 summarizes the dihedral angles of Trp side chains, χ_1 and χ_2, in the presence and absence of halothane. It seems that the dihedral angles in the presence of halothane have greater standard deviations, which could be interpreted to imply that the Trp side-chain conformational mobility is much higher in the system with halothane. Such increased flexibility of the Trp side chain might be induced by the anesthetic disruption of hydrogen bonding between the tryptophan indole and the phosphate oxygen in the lipid head region or the fatty acid oxygen near the glycerol bridge lipids.[22]

Figure 8 depicts the much larger sweeping range of the χ_2 of Trp^{15} in the presence halothane. The averaged values of χ_2 of Trp^{15} also differ considerably in systems with and without halothane. The same phenomenon is observable on Trp^{11}, as indicated in Table 1. The orientations of Trp^{11} and Trp^{15} in the presence of halothane make their dipole more parallel to the channel axis, and consequently promote Na^+ permeation.

In conclusion, we have calculated the PMF for Na^+ permeation across the gA channel using SMD simulations. The profiles of PMF allow for semiquantitative assessment of the ion-binding site, binding energies, and central barrier height. The results are in reasonable agreement with previous experimental and computational studies. The halothane effect on the PMF is too subtle to be accurately quantified, considering the limitations on the accuracy of the PMF inherited from the employment of a nonpolarizable force field and the periodical boundary

condition. Nevertheless, we have demonstrated that the quality of results from SMD simulations in this study is at least internally consistent. Most significantly, the level of atomic details contained in the results, when taken together, underscores the importance of dynamic (entropic) properties instead of static equilibrium (enthalpic) properties in triggering ion permeation. While the height of the energy barrier determines the ion equilibration across the membrane, the actual transport event is a dynamic process dependent upon the probability of concerted carbonyl bond flickering to provide Na^+ coordination from one energy well to the next in a relay. Consistent with our previous experimental studies, the anesthetic interaction with the anchoring Trp side chains increases the chance of Trp side-chain reorientation, triggering more frequent hopping from the ion-binding site to initiate the permeation process. These promising results warrant the further development of the SMD method for more quantitative analysis of transport across ion channels in general.

Acknowledgment. This research was facilitated through an allocation of advanced computing resources at the Pittsburgh Supercomputing Center through the support of the National Science Foundation and the Commonwealth of Pennsylvania. This research was supported in part by grants from the National Institutes of Health (R01GM066358, R01GM056257, and R37GM049202).

References and Notes

(1) Arseniev, A. S.; Barsukov, I. L.; Bystrov, V. F.; Lomize, A. L.; Ovchinnikov, Yu. A. *FEBS Lett.* **1985**, *186*, 168.
(2) Ketchem, R. R.; Hu, W.; Cross, T. A. *Science* **1993**, *261*, 1457.
(3) Cross, T. A. *Methods Enzymol.* **1997**, *289*, 672.
(4) Mueller, P.; Rudin, D. O.; Tien, H. T.; Wescott, W. C. *Nature* **1962**, *194*, 979.
(5) Andersen, O. S.; Koeppe, R. E., II. *Physiol. Rev.* **1992**, *72*, S89.
(6) Miloshevsky, G. V.; Jordan, P. C. *Trends Neurosci.* **2004**, *27*, 308.
(7) Andersen, O. S.; Koeppe, R. E., II.; Roux, B. *IEEE Trans Nanobiosci.* **2005**, *4*, 10.
(8) Roux, B.; Karplus, M. *J. Am. Chem. Soc.* **1993**, *115*, 3250.
(9) Busath, D. D. *Annu. Rev. Physiol.* **1993**, *55*, 473.
(10) Dorman, V. L.; Jordan, P. C. *Biophys. J.* **2004**, *86*, 3529.
(11) Jordan, P. C. *Biophys. J.* **1990**, *58*, 1133.
(12) Allen, T. W.; Bastug, T.; Kuyucak, S.; Chung, S. H. *Biophys. J.* **2003**, *84*, 2159.
(13) Allen, T. W.; Andersen, O. S.; Roux, B. *Proc. Natl. Acad. Sci. U.S.A.* **2004**, *101*, 117.
(14) Israelewitz, B.; Gao, M.; Schulten, K. *Curr. Opin. Struct. Biol.* **2001**, *11*, 224.
(15) Krammer, A.; Lu, H.; Isralewitz, B.; Schulten, K.; Vogel, V. *Proc. Natl. Acad. Sci. U.S.A.* **1999**, *96*, 1351.
(16) Tajkhorshid, E.; Nollert, P.; Jensen, M. O.; Miercke, L. J.; O'Connell, J.; Stroud, R. M.; Schulten, K. *Science* **2002**, *296*, 525.
(17) Jensen, M. O.; Park, S.; Tajkhorshid, E.; Schulten, K. *Proc. Natl. Acad. Sci. U.S.A.* **2002**, *99*, 6731.
(18) Tang, P.; Eckenhoff, R. G.; Xu, Y. *Biophys. J.* **2000**, *78*, 1804.
(19) Tang, P.; Hu, J.; Liachenko, S.; Xu, Y. *Biophys. J.* **1999**, *77*, 739.
(20) Tang, P.; Mandal, P. K.; Zegarra, M. *Biophys. J.* **2002**, *83*, 1413.
(21) Tang, P.; Simplaceanu, V.; Xu, Y. *Biophys. J.* **1999**, *76*, 2346.
(22) Tang, P.; Xu, Y. *Proc. Natl. Acad. Sci. U.S.A.* **2002**, *99*, 16035.
(23) Liu, Z.; Xu, Y.; Tang, P. *Biophys. J.* **2005**, *88*, 3784.
(24) Ketchem, R.; Roux, B.; Cross, T. *Structure* **1997**, *5*, 1655.
(25) Nosé, S. *J. Chem. Phys.* **1984**, *81*, 511.
(26) Hoover, W. G. *Phys. Rev. A* **1985**, *31*, 1695.
(27) Darden, T.; York, D.; Pedersen, L. *J. Chem. Phys.* **1993**, *98*, 10089.
(28) Van Gunsteren, W. F.; Berendsen, H. J. C. *Mol. Phys.* **1977**, *34*, 1311.
(29) Kale, L.; Skeel, R.; Bhandarkar, M.; Brunner, R.; Gursoy, A.; Krawetz, N.; Phillips, J.; Shinozaki, A.; Varadarajan, K.; Schulten, K. *J. Comput. Phys.* **1999**, *151*, 283.
(30) Brooks, B. R.; Bruccoleri, R. E.; Olafson, B. D.; States, D. J.; Swaminathan, S.; Karplus, M. *J. Comput. Chem.* **1983**, *4*, 187.
(31) MacKerell, A. D. *Abstr. Pap. Am. Chem. Soc.* **1998**, *216*, 042.
(32) Humphrey, W.; Dalke, A.; Schulten, K. *J. Mol. Graphics* **1996**, *14*, 33.
(33) Roux, B. *Biophys. J.* **1999**, *77*, 139.
(34) Jarzynski, C. *Phys. Rev. Lett.* **1997**, *78*, 2690.
(35) Park, S.; Schulten, K. *J. Chem. Phys.* **2004**, *120*, 5946.
(36) Hunt, G. R. A.; Veiro, J. A. *Biochem. Soc. Trans.* **1986**, *14*, 602.
(37) Urry, D. W.; Prasad, K. U.; Trapane, T. L. *Proc. Natl. Acad. Sci. U.S.A.* **1982**, *79*, 390.
(38) Olah, G. A.; Huang, H. W.; Liu, W. H.; Wu, Y. L. *J. Mol. Biol.* **1991**, *218*, 847.
(39) Woolf, T. B.; Roux, B. *Biophys. J.* **1997**, *72*, 1930.
(40) Levitt, D. G. *Annu. Rev. Biophys. Biophys. Chem.* **1986**, *15*, 29.
(41) Sham, S. S.; Shobana, S.; Townsley, L. E.; Jordan, J. B.; Fernandez, J. Q.; Andersen, O. S.; Greathouse, D. V.; Hinton, J. F. *Biochemistry* **2003**, *42*, 1401.
(42) Russell, E. W.; Weiss, L. B.; Navetta, F. I.; Koeppe, R. E., II.; Andersen, O. S. *Biophys. J.* **1986**, *49*, 673.
(43) Jakobsson, E.; Chiu, S. W. *Biophys. J.* **1987**, *52*, 33.
(44) Bostick, D.; Berkowitz, M. L. *Biophys. J.* **2003**, *85*, 97.
(45) Cross, T. A.; Tian, F.; Cotten, M.; Wang, J.; Kovacs, F.; Fu, R. *Novartis Found. Symp.* **1999**, *225*, 4.
(46) Tian, F.; Cross, T. A. *J. Mol. Biol.* **1999**, *285*, 1993.
(47) Mackay, D. H.; Berens, P. H.; Wilson, K. R.; Hagler, A. T. *Biophys. J.* **1984**, *46*, 229.
(48) Roux, B.; Woolf, T. B. *Novartis Found. Symp.* **1999**, *225*, 113.
(49) Jordan, P. C. *J. Gen. Physiol.* **1999**, *114*, 601.
(50) Elber, R.; Chen, D. P.; Rojewska, D.; Eisenberg, R. *Biophys. J.* **1995**, *68*, 906.
(51) Tian, F.; Lee, K. C.; Hu, W.; Cross, T. A. *Biochemistry* **1996**, *35*, 11959.
(52) Wallace, B. A. *Adv. Exp. Med. Biol.* **1996**, *398*, 607.
(53) Koeppe, R. E., II.; Mazet, J. L.; Andersen, O. S. *Biochemistry* **1990**, *29*, 512.
(54) Daumas, P.; Heitz, F.; Ranjalahy-Rasoloarijao, L.; Lazaro, R. *Biochimie* **1989**, *71*, 77.
(55) Busath, D. D.; Thulin, C. D.; Hendershot, R. W.; Phillips, L. R.; Maughan, P.; Cole, C. D.; Bingham, N. C.; Morrison, S.; Baird, L. C.; Hendershot, R. J.; Cotten, M.; Cross, T. A. *Biophys. J.* **1998**, *75*, 2830.
(56) Andersen, O. S.; Greathouse, D. V.; Providence, L. L.; Becker, M. D.; Koeppe, R. E., II. *J. Am. Chem. Soc.* **1998**, *120*, 5142.